Vibrational Force Field Calculations of Ara-A. Application to the Analysis of Its Infrared and Raman Spectra

Belén Hernández,[†] Abdelaziz Elass,[‡] Raquel Navarro,[†] Gérard Vergoten,[‡] and Antonio Hernanz*,[†]

Departamento de Ciencias y Técnicas Fisicoquímicas, Universidad Nacional de Educación a Distancia (UNED), Senda del Rey s/n, E-28040 Madrid, Spain, and CRESIMM, Université des Sciences et Technologies de Lille I, UFR de Chimie, Bât. C8, 1er ét. 59655 Villeneuve d'Ascq Cedex, France

Received: December 4, 1997; In Final Form: March 13, 1998

The vibrational spectra of the arabinonucleoside 9-β-D-arabinofuranosyladenine, ara-A, are reported. Ara-A is of interest because of its antiviral activity. An accurate knowledge of the vibrational modes is a valuable help for the elucidation of drug−nucleotide and drug−enzyme interactions. The FTIR and FT-Raman spectra of ara-A were recorded from 4000 to 30 cm^{-1}. A hexadeuterated derivative (deuteration at C8, the amino and hydroxyl groups) was synthesized, and its spectra were also used for the vibrational analysis of ara-A. Theoretical frequencies as well as the potential energy distribution of the vibrational modes of ara-A were calculated using the ab initio HF/3-21G method, the semiempirical PM3 method, and two valence force fields. The results obtained are compared in order to show the accuracy and reliability of each method. The observed spectra and the vibrational frequencies of ara-A are assigned considering the potential energy distributions and the observed band shifts by deuteration. Scaled ab initio and PM3 frequencies are in a good agreement with the experimental data. The valence force field was found to reproduce them with enough accuracy when a large set of harmonic force constants is used. Previous normal coordinate analyses of the adenine and related molecules are compared with these results.

Introduction

Nucleoside analogues are an important group of antiviral drugs. Arabinosides have attracted great attention owing to their antiviral activity of broad spectrum against DNA viruses and RNA tumor viruses (oncoviruses). The arabinonucleosides differ from their ribo and deoxyribo analogues in the bonds at the C2′ position. The hydroxyl group is cis-oriented to the glycosidic C1′−N9 bond, this group is trans in ribonucleosides, and no hydroxyl group exists in this position for deoxyribonucleosides. These changes have small effects on the bond lengths and angles of the furanose ring, keeping a similar puckering range.[1]

Adenine arabinoside, 9-*beta*-D-arabinofuranosyledenine (vidarabine or ara-A), Figure 1, is a purine nucleoside, synthesized in the early 1960s,[2] active against DNA viruses of the herpes group.[3−6] Ara-A is an effective chemotherapeutic agent[3,7−10] used in combination with inhibitors of adenosine deaminase.[3,8] The compound is curative against L 1210 leukemia in mice[11] and for several types of mammalian tumors.[12] Some studies have indicated that the mechanism involves the phosphorylation of ara-A by cellular kinases to active 5′-triphosphate,[8,13] which has been proved to inhibit the viral DNA polymerase.[14]

X-ray diffraction studies of this compound were performed by Bunick and Voet,[15] who observed orthorhombic crystals with unit cell dimensions $a = 5.08$ Å, $b = 10.485$ Å, $c = 21.419$ Å and four molecules per unit cell. There are infinite stacks of adenine residues in which neighboring rings are related by the *"a"* axis. The arabinose puckering for ara-A is $^3T_4$, one of the preferred puckering modes for the ribose ring. Hence, the sugar

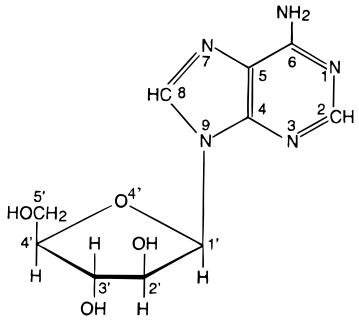

Figure 1. Numbering of atoms in ara-A.

conformation of ara-A is quite similar to that of adenosine.[16] Both molecules are C3′-endo, gauche−trans oriented about their C4′−C5′ exocyclic bond and within the orientation range anti about the glycosidic bond. The conformational similarities between ara-A and adenosine are such that ara-A is accepted into many biosynthetic pathways that normally incorporate adenosine. Several authors[12,17,18] have suggested that once ara-A is included into various biomolecules, the configurational differences between adenosine and ara-A render these aggregates partially or even totally inactive in their biochemical processes. An accurate knowledge of the vibrational modes of this arabinonucleoside would be an important help for the elucidation of drug−target interactions.

Raman spectra of ara-A, ara-A·HCl, adenosine and adenosine hydrochloride have been reported by Theophanides et al.,[19] but the region around 3000 cm^{-1} was not recorded. The observed frequencies were assigned on the basis of correlated group frequencies. In the present work, the vibrational study is extended to infrared and Raman spectroscopy (4000−30 cm^{-1})

[†] Universidad Nacional de Educación a Distancia.
[‡] CRESIMM.

S1089-5647(98)00425-8 CCC: $15.00 © 1998 American Chemical Society
Published on Web 05/06/1998

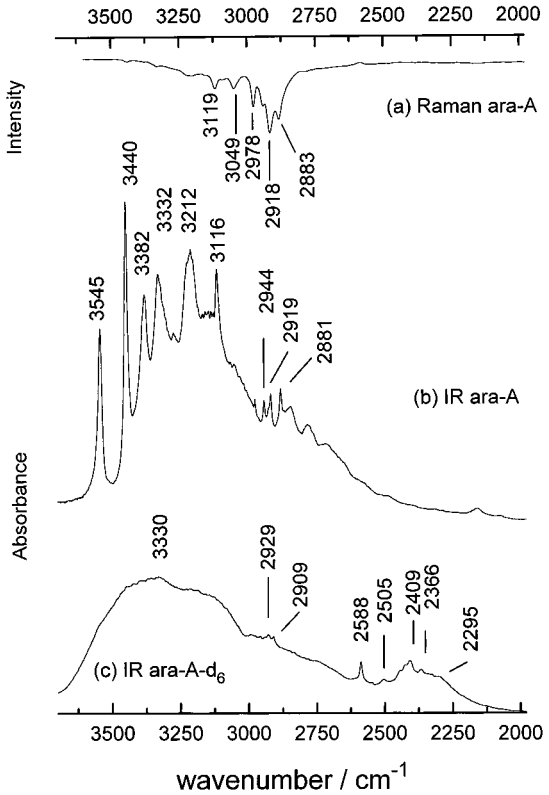

Figure 2. 3500−2000 cm^{-1} spectral region. (a) FT-Raman spectrum of ara-A; (b) FTIR spectrum of ara-A; (c) FTIR spectrum of ara-A-d_6.

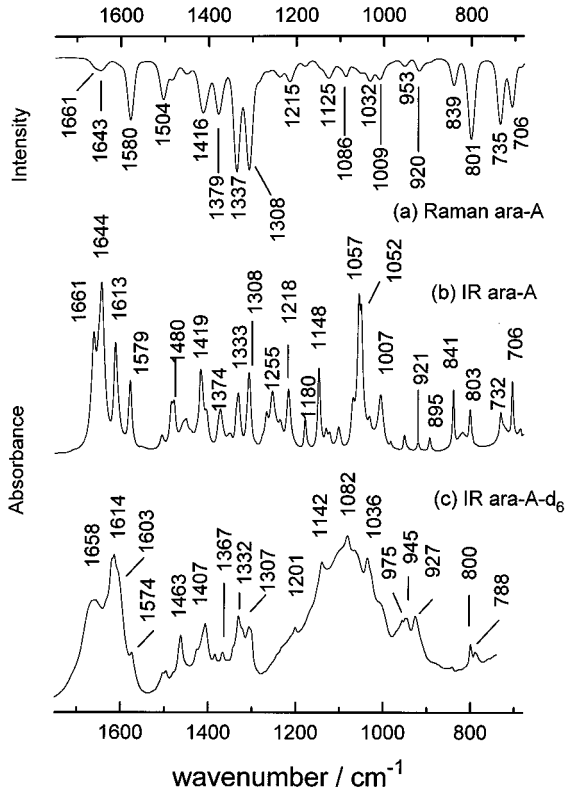

Figure 3. 1700−700 cm^{-1} spectral region. (a) FT-Raman spectrum of ara-A. (b) FTIR spectrum of ara-A; (c) FTIR spectrum of ara-A-d_6.

for ara-A and a hexadeuterated derivative, ara-A-d_6 (deuteration at C8, the amino and hydroxyl groups), synthesized for this purpose. The assignment of the vibrational spectra of ara-A is based on normal coordinate treatments using the ab initio HF/3-21G method, the semiempirical PM3 method, and two different valence force fields: one built transferring force constants from related molecules and the other using the force constants obtained from the ab initio calculation of ara-A molecule reported here. The results obtained from all these treatments are compared to evaluate their reliability. They are also compared with previous normal coordinate analyses of related molecules.[19−30]

Experimental Section

Materials and Instrumentation. Adenine 9-β-D-arabinofuranoside was purchased from Sigma Chemical Co. and used as supplied. The ara-A-d_6 isotopomer (deuteration at C8, the amino and hydroxyl groups) was obtained heating a solution of ara-A in ^2H_2O at 80 °C for 20 h and subsequent recrystallization. Deuteration was confirmed by ^1H NMR spectroscopy.

The FTIR spectra were recorded in a Bomem-DA3 interferometer, working under vacuum (pressure ≤ 133.3 Pa). The mid-infrared spectra of polycrystalline ara-A and ara-A-d_6 in KBr pellets, Figures 2 and 3, were recorded coadding 500 interferograms with an effective apodized resolution $s = 0.89$ cm^{-1} (RES = 1.0 and Hamming apodizing function). A DTGS/MIR detector, a Globar source, and a KBr beam splitter were used. Far-infrared, FIR, spectra of ara-A and ara-A-d_6 in polyethylene pellets, from 700 to 200 cm^{-1} and from 200 to 40 cm^{-1}, Figure 4, were obtained coadding 1000 interferograms, $s = 1.77$ cm^{-1} (RES = 2 and Hamming apodizing function) using a DTGS/FIR detector and a high-pressure mercury lamp. Mylar beam splitters of 3 and 12 μm were used for the former and the latter far-IR regions, respectively.

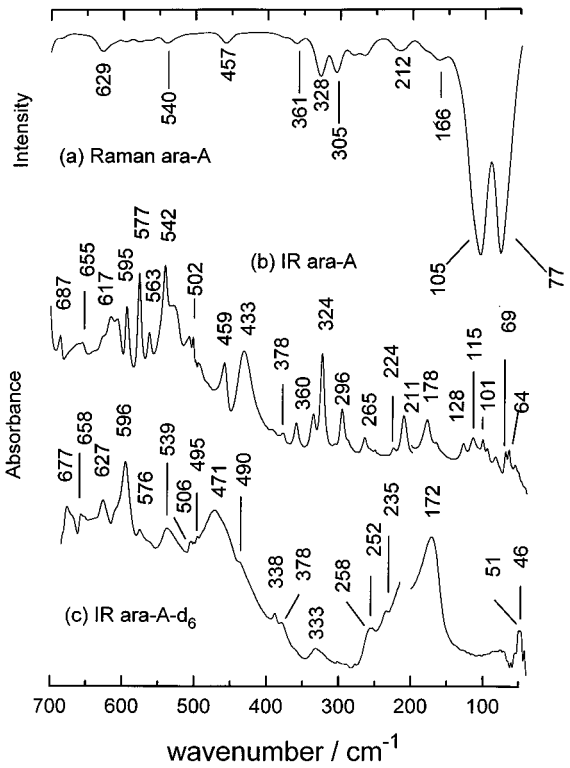

Figure 4. 700−30 cm^{-1} spectral region. (a) FT-Raman spectrum of ara-A. (b) FTIR spectrum of ara-A; (c) FTIR spectrum of ara-A-d_6.

The FT-Raman spectra of the polycrystalline ara-A were recorded using a Bruker Raman RFS 100 spectrometer. A Krypton discharge lamp pumped Nd^{3+}:YAG laser working at 1064 nm was the exciting source. Raman emission was collected at 180°, i.e., with backscattering geometry.A quartz beam splitter and a germanium detector working at 77 K (cooled

TABLE 1: Internal Coordinates Definition (ν = Stretching, δ = In-Plane Bending, π = Out-of-Plane Bending, τ = Torsion)

Bioviban A: Internal Coordinates for the Ara-A Molecule

1 ν N1−C2	34 ν O5′−H	67 δ C3′−C4′−O4′	100 τ C2−N3−C4−C5
2 ν N1−C6	35 δ N1−C2−N3	68 δ C4′−O4′−C1′	101 τ N3−C4−C5−C6
3 ν C2−H	36 δ C2−N3−C4	69 δ H−C2′−C3′	102 τ C4−C5−C6−N1
4 ν C2−N3	37 δ N3−C4−C5	70 δ C2′−C3′−O3′	103 τ C5−C6−N1−C2
5 ν N3−C4	38 δ C4−C5−C6	71 δ C3′−C2′−O2′	104 τ C5−C4−N9−C8
6 ν C4−C5	39 δ C5−C6−N1	72 δ O2′−C2′−H	105 τ C4−N9−C8−N7
7 ν N9−C4	40 δ C6−N1−C2	73 δ C2′−O2′−H	106 τ N9−C8−N7−C5
8 ν C5−C6	41 δ N7−C5−C4	74 δ H−C3′−C2′	107 τ C8−N7−C5−C4
9 ν C5−N7	42 δ C5−N7−C8	75 δ O3′−C3′−C4′	108 τ N1−C6−N7−H22
10 ν C6−N6	43 δ N7−C8−N9	76 δ C4′−C3′−H	τ N1−C6−N7−H23
11 ν N6−H	44 δ C8−N9−C4	77 δ H−C4′−C3′	109 τ C4−N9−C1′−O4′
12 ν N6−H′	45 δ N1−C2−H	78 δ C3′−C4′−C5′	110 τ C2′−C1′−O4′−C4′
13 ν N7−C8	46 δ N3−C2−H	79 δ H−C3′−O3′	111 τ O4′−C1′−C2′−C3′
14 ν C8−H	47 δ N3−C4−N9	80 δ C3′−O3′−H	112 τ C1′−C2′−C3′−C4′
15 ν N9−C8	48 δ C4−N9−C1′	81 δ H−C4′−C5′	113 τ C2′−C3′−C4′−O4′
16 ν N9−C1′	49 δ O4′−C1′−N9	82 δ C4′−C5′−H	114 τ C3′−C4′−O4′−C1′
17 ν C1′−H	50 δ N9−C1′−C2′	83 δ C4′−C5′−H′	115 τ HO2′−O2′−C2′−H2′
18 ν C1′−O4′	51 δ N9−C1′−H	84 δ C4′−C5′−O5′	116 τ H3′−C3′−O3′−HC3′
19 ν C2′−C1′	52 δ C8−N9−C1′	85 δ H−C5′−H′	117 τ HC4′−C4′−C5′−O5′
20 ν C4′−O4′	53 δ N9−C8−H	86 δ H−C5′−O5′	118 τ C4′−C5′−O5′−HO5′
21 ν C2′−O2′	54 δ H−C8−N7	87 δ H′−C5′−O5′	119 δ C5′−C4′−O4′
22 ν C2′−C3′	55 δ N7−C5−C6	88 δ C5′−O5′−H	
23 ν C2′−H	56 δ C5−C6−N6	89 δ C5−C4−N9	
24 ν O2′−H	57 δ C6−N6−H	90 δ O4′−C4′−H	
25 ν C3′−O3′	58 δ H−N6−H′	91 δ O4′−C1′−H	
26 ν O3′−H	59 δ C6−N6−H	92 π H−C8−N7−N9	
27 ν C3′−C4′	60 δ N1−C6−N6	93 π H−C2−N1−N3	
28 ν C3′−H	61 δ O4′−C1′−C2′	94 π N6−C6−N1−C5	
29 ν C4′−C5′	62 δ C2′−C1′−H′	95 π H−N6−N1−C5	
30 ν C4′−H	63 δ O2′−C2′−C1′	96 π H′−N6−N1−C5	
31 ν C5′−O5′	64 δ C1′−C2′−H	97 π N9−C1′−C4−C8	
32 ν C5′−H	65 δ C1′−C2′−C3′	98 τ C6−N1−C2−N3	
33 ν C5′−H′	66 δ C2′−C3′−C4′	99 τ N1−C2−N3−C4	

Bioviban B, ab Initio HF/3−21G and PM3 Out−of−Plane Bends

π N1−C5C6N6 (opb $N1_1$)	π C5−N3C4N9 (opb $C5_1$)	π N9−N7C8H (opb $N9_1$)
π N1−N3C2H (opb $N1_2$)	π C5−C6N1N6 (opb $C5_2$)	π N9−N3C4C5 (opb $N9_2$)
π N3−N1C2H (opb $N3_1$)	π N7−C4C5C6 (opb $N7_1$)	π C1′−N1N9C8 (opb C1′)
π N3−C5C4N9 (opb $N3_2$)	π N7−N9C8H (opb $N7_2$)	π N6−N1C5C6 (opb N6)
π C4 −C5C6N7 (opb $C4_1$)	π C8−C4N9C1′ (opb C8)	π H−C2N1N3 (opb H−C2)
π C4 −C8N9C1′ (opb $C4_2$)	π H−C8N9N7 (opb H−C8)	

by liquid N_2) were used to obtain the FT-Raman spectrum, Figures 2a−4a. One hundred interferograms were coadded, with a nominal resolution of 8 cm^{-1} after Blackman−Harris apodization.

Normal Coordinate Treatments

Ab Initio and PM3 Treatments. Ab initio at level HF, using the basis set 3-21G, and PM3 molecular orbital calculations were carried out using both methods as implemented in Gaussian 94.[31] Total geometry optimizations, ab initio and PM3, were performed using the crystalline structure obtained from X-ray data[15] as initial geometry. After each change of atomic coordinates, the energy of the fundamental state of the system was evaluated by the self-consistent field, SCF (ab initio and PM3), using the restricted Hartree−Fock, RHF, spin-pairing treatment without configuration interaction. The optimizations are completed when the maximum force, rms force, maximum displacement, and rms displacement were less than 0.000 450, 0.000 300, 0.001 800, and 0.001 200 internal units (hartrees−bohrs−radians), respectively. The optimized geometries and force constants resulting from the second derivatives of the energies have been used to compute the wavenumbers corresponding to the normal modes. The force fields were scaled applying the Redong program.[32]

Valence Force Field. The normal coordinate treatment based on the Wilson's GF method[33] was applied to ara-A with some specific details. The molecular geometry to built the G matrix was taken from crystallographic data.[15] This matrix was written in internal coordinates representation, using an extended basis set of 119 coordinates, Table 1, including 29 redundancies which were eliminated by diagonalization, as their corresponding eigenvalues are zero. The GF product results in the secular equation, whose eigenvalues yield the 90 harmonic vibration wavenumbers (32 atoms). A complete set of valence force constants for the ara-A molecule was not found in the literature until now. Nevertheless, the overlay technique has proved to be a reasonable approach.[29,30,34−36] Thus, a valence force field with 119 diagonal force constants and 237 off-diagonal terms was built from force constants published for adenine,[20] assumed to be valid for the base residue: from guanine and 5′-dGMP[34] for the glycosidic bond and C−N−H bonds, from 5'-dGMP[34] and tetrahydrofuran (THF)[37] for the arabinose moiety, Tables 2 and 3.

The second force field was built using the resulting F matrix from our ab initio calculation. In this case, a set of 130 internal coordinates was used. In this case, the out-of-plane bends, opb's (92 to 97), have been replaced by the opb's listed in Table 1. This has been done in order to be coherent with the definition in the ab initio treatment. The 130 diagonal force constants and the 2102 off-diagonal elements were transferred from the ab initio F matrix, Table 1S. Calculations with the first and second force field, Bioviban A and B, respectively, have been done using the program Bioviban developed by this research

TABLE 2: Bioviban A: Diagonal Valence Force Constants (In-Plane and Out-of-Plane Modes) for the Set of 119 Internal Coordinates for Ara-A, Transferred from Values Published for Adenine (Dhaouadi et al.[20]), Guanine (Majoube[25]), 5′-dGMP (Ghomi and Taillandier[34]), and Tetrahydrofuran (Eyster and Prohofsky[37]). Units: Stretching Force Constants (mdyn Å^{-1}), Bending Force Constants (mdyn Å), Out-of-Plane Bending, and Torsional Force Constants (mdyn)

			Stretch				
1	6.21	10	6.2	19	4.2697	28	4.5709
2	6.2	11	5.86	20	5.4953	29	4.652
3	5.13	12	5.86	21	4.745	30	4.6440
4	6.88	13	7.0	22	4.2697	31	4.342
5	6.4	14	5.41	23	4.5709	32	4.644
6	6.4	15	5.92	24	5.534	33	4.644
7	5.92	16	4.86	25	4.745	34	5.534
8	5.73	17	4.6440	26	5.534		
9	5.51	18	5.4953	27	4.2697		
			Bend				
35	1.53	50	1.588	65	1.0079	80	0.530
36	1.9	51	0.5017	66	1.0079	81	0.7346
37	1.23	52	1.380	67	1.1633	82	0.7346
38	1.0	53	0.425	68	1.3081	83	0.7346
39	1.29	54	0.425	69	0.656	84	0.1633
40	1.998	55	1.350	70	1.1633	85	0.5017
41	1.23	56	1.44	71	1.1633	86	0.781
42	1.68	57	0.415	72	0.718	87	0.781
43	1.39	58	0.452	73	0.530	88	0.530
44	1.4	59	0.415	74	0.656	89	1.6
45	0.52	60	1.28	75	1.1633	90	0.781
46	0.52	61	1.1633	76	0.656	91	0.781
47	1.0	62	0.7346	77	0.7346	119	1.1633
48	1.380	63	1.1633	78	1.0079		
49	1.363	64	0.656	79	0.781		
			Wag				
92	0.362	93	0.3	94	0.43	95	0.0044
96	0.0044	97	0.43				
			Torsion				
98	0.257	104	0.55	110	0.0101	116	0.010
99	0.43	105	0.55	111	0.0208	117	0.010
100	0.257	106	0.61	112	0.0208	118	0.010
101	0.585	107	0.55	113	0.0208		
102	0.455	108	0.0935	114	0.0101		
103	0.43	109	0.1	115	0.010		

group[16,18] and modified for its application to biological systems.[29,30]

Results

The optimized ab initio geometry is closer to the crystalline structure[15] than the geometry obtained from PM3, Table 4. The bond distances are similar to the experimental data except for C1′−N9, which lengthen from 1.48 to 1.53 Å in the PM3 optimized structure and shorten to 1.43 Å in the ab initio structure. Concerning the arabinose ring, the ab initio treatment keeps a degree of pucker similar to those found by X-ray diffraction; PM3 tends to systematically produce sugar rings closer to planarity. Table 4 lists the geometrical parameters of the three mentioned structures.

The spectra of ara-A and ara-A-d_6 are shown in Figures 2−5. The wavenumber of fundamentals and the potential energy distributions, PEDs, calculated by ab initio, PM3, and Bioviban (A and B) treatments as well as the observed wavenumbers are listed in Tables IIS and IIIS. Most of the scale factors take values between 0.95 and 0.80. The lowest value, 0.65, corresponds to four torsions. The standard deviation between calculated and observed wavenumbers for the ab initio treatment is 6.16 cm^{-1}, whereas for the PM3 calculation it is 12.0 cm^{-1} (the largest deviations being localized on C8H, C2H, C4′H, and C2′H stretching frequencies; a standard deviation of 6.74 cm^{-1} is obtained without considering these frequencies). No force field refinement has been done on Bioviban treatments. Assignments proposed by the different methods are discussed and compared.

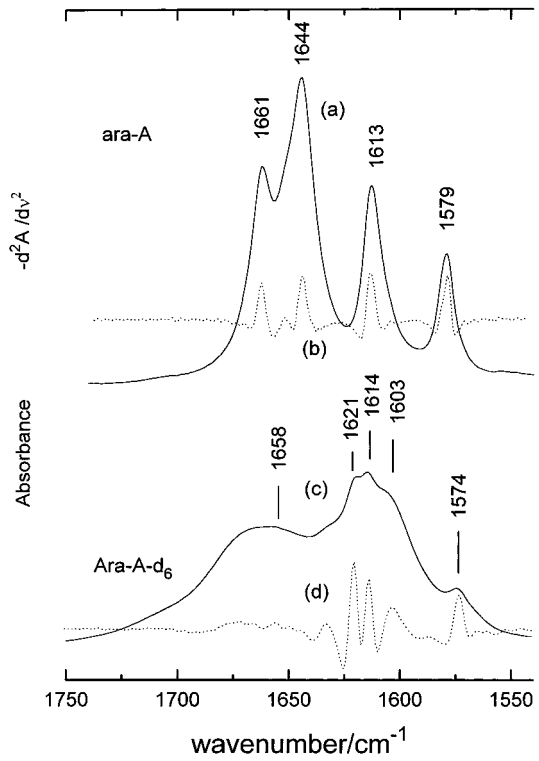

Figure 5. Comparison between the FTIR spectra of ara-A and ara-A-d_6 in the region 1750−1550 cm^{-1}. Second derivative spectra in dots.

Discussion

The assignment of the observed bands is discussed by spectral regions considering the nature of the normal modes.

3550−2000 cm^{-1}. Intense IR bands appear in this region due to N−H, O−H, and C−H stretching vibrations. The two intense bands at 3545 and 3450 cm^{-1} are attributed to the antisymmetric and symmetric N−H stretching modes, $\nu_a(NH_2)$ and $\nu_s(NH_2)$, respectively, in agreement with previous studies for adenine, adenosine, and ara-A·HCl[20,21,24,29,30] and the results of the ab initio, PM3, and Bioviban calculations. These bands shift by deuteration to lower wavenumbers in the neighborhood of ≈2600 cm^{-1}. The broad IR bands observed at 3382, 3332, and 3212 cm^{-1} are due to the stretching modes of the hydroxyl groups ν(O2′H), ν(O3′H), and ν(O5′H), respectively. The broadening of these bands suggests that these groups are involved in hydrogen bonds, as indicated by Bunick and Voet[15] from X-ray diffraction data. This group of bands shifts by deuteration to the region of ≈2500−2300 cm^{-1}. The ν(CH) bands overlap with the ν(OH) bands in the IR spectrum. The ν(C8H) and ν(C2H) stretching modes appear at wavenumbers ≈ 3000 cm^{-1}, in agreement with published values for adenine, adenosine, and ara-A·HCl.[20,21,24,29,30] The IR band at 3116 cm^{-1} is assigned to the ν(C8H) mode; it shifts upon deuteration to 2290 cm^{-1}. The C−H sugar stretches are observed at lower wavenumbers, 2900−2800 cm^{-1}. Concerning the Bioviban calculations, we found in this spectral region that the calculation B reproduces very well the observed wavenumbers, while calculation A seems less suitable.

1700−1000 cm^{-1}. The bands in this region are mainly due to in-plane base[19−24,26,28,38] and sugar vibrations. Calculations

TABLE 3: Bioviban A: Off-Diagonal Valence Force Constants (In-Plane and Out-of-Plane Modes) for the Set of 119 Internal Coordinates for Ara-A, Transferred from Values Published for Adenine (Dhaouadi et al.[20]), Guanine (Majoube[25]), 5′-dGMP (Ghomi and Taillandier[34]), and Tetrahydrofuran (Eyster and Prohofsky[37]). Units: Stretching Force Constants (mdyn Å^{-1}), Bending Force Constants (mdyn Å), Out-of-Plane Bending, and Torsional Force Constants (mdyn)

Adenine and Glycoside Bond							
Stretch−Stretch (In-Plane)							
1−2	0.641	2−13	0.22	5−8	−0.15	7−8	0.15
1−4	0.5	2−8	0.65	5−7	0.2	8−10	0.75
1−6	0.35	2−5	0.2	6−8	0.44	8−9	−0.15
1−5	0.2	4−13	−0.17	6−9	0.15	9−13	0.9
1−8	−0.15	4−6	−0.15	6−7	0.15	13−15	0.9
2−4	0.15	4−5	0.25	6−13	0.15	15−16	0.2
2−6	0.35	4−8	0.65	7−15	0.2	7−16	0.2
2−10	0.801	5−6	0.35	7−13	−0.71	16−19	−0.15
Bend−Bend (In-Plane)							
60−39	0.39	56−55	−0.45	56−60	0.25	57−56	0.2
56−39	−0.1	59−60	0.25	59−56	0.2		
Stretch−Bend (In-Plane)							
1−35	0.701	5−36	0.701	8−38	0.2	13−43	0.58
1−40	0.701	5−37	0.701	8−39	0.2	15−43	0.55
1−45	0.54	5−47	0.55	8−55	−0.3	15−44	0.8
2−39	6.2	6−37	0.3	9−42	0.75	15−53	0.76
2−40	0.4	6−38	0.75	9−55	0.75	15−48	−0.03
2−60	0.78	6−89	0.3	10−39	0.901	15−52	−0.03
4−35	0.75	7−89	0.9	10−40	0.901	16−44	−0.03
4−36	0.75	7−44	0.9	10−38	0.901	16−89	−0.03
4−46	0.35	7−47	0.55	13−42	0.58	16−43	−0.03
Wag−Wag (Out-of-Plane)							
95−94	−0.03	96−94	−0.062	92−93	0.02	94−93	−0.01
Wag−Torsion (Out-of-Plane)							
92−105	0.12	92−106	−0.245	93−98	0.115	93−99	−0.06
94−102	0.14	94−103	0.11				
Torsion−Torsion (Out-of-Plane)							
104−105	0.195	105−101	−0.05	108−103	−0.01	102−101	−0.08
104−106	−0.05	104−107	−0.14	99−100	−0.04	103−99	0.09
101−100	−0.12	105−106	0.035	98−99	0.0625	103−101	−0.08
105−107	0.05	107−101	0.1	98−103	0.02	99−101	−0.01
106−101	0.12	101−104	0.22	102−103	0.05	100−102	0.195
Deoxyribose Ring and Glycosidic Bond							
Stretch−Stretch							
18−20	0.2956	19−22	0.101	22−27	0.101	27−20	0.101
18−19	0.1016	21−22	0.101	25−27	0.101	29−31	0.101
19−21	0.101	22−25	0.101	27−29	0.101	33−32	−0.0652
Bend−Bend							
49−61	−0.041	66−74	−0.052	69−74	−0.021	78−119	0.1139
61−91	−0.031	66−76	−0.052	70−74	0.0158	81−82	−0.0881
61−68	0.285	66−69	−0.052	70−79	−0.031	81−83	−0.0881
61−62	0.0158	66−77	−0.031	71−72	−0.031	81−84	0.0158
61−65	0.1139	66−71	0.1139	71−74	0.0158	81−90	0.0363
61−64	0.0158	66−70	0.1139	74−76	0.012	81−119	0.158
63−72	−0.031	66−75	0.1139	74−79	0.0363	82−83	−0.0881
63−62	0.0158	66−67	0.1139	75−76	0.0158	82−84	0.0158
63−65	0.1139	66−78	0.1139	75−77	0.0158	82−87	0.0363
63−64	0.0158	67−78	0.1139	75−78	0.1139	82−119	0.0158
62−65	−0.031	67−76	0.0158	75−79	−0.031	83−84	0.0158
62−64	0.0314	67−77	0.0158	76−77	−0.0664	83−119	0.0158
64−65	−0.052	67−90	−0.031	76−78	−0.052	83−86	0.0363
64−69	−0.021	67−68	0.0285	76−79	0.0363	84−86	−0.031
64−72	0.0363	68−119	0.0285	77−78	−0.031	84−87	−0.031
65−71	0.1139	68−90	0.0844	77−90	0.0363	86−87	−0.0824
65−74	−0.052	68−91	0.0844	78−81	−0.031	90−119	−0.031
65−66	0.1139	69−70	0.0158	78−82	−0.031		
65−69	−0.152	69−71	0.0158	78−83	−0.031		
65−70	0.1139	69−72	0.0363	78−84	0.1139		
Stretch−Bend							
16−49	0.347	20−67	0.4197	22−66	0.417	27−77	0.4288
16−50	0.347	20−119	0.4197	22−65	0.417	29−119	0.3656
18−61	0.4197	20−68	0.8257	25−79	0.3842	29−84	0.3656
18−68	0.8752	20−90	0.3842	25−75	0.4197	29−78	0.417
18−91	0.3842	21−63	0.4197	25−70	0.4197	29−81	0.4288
19−61	0.3656	21−71	0.4197	27−66	0.417	29−82	0.4281
19−63	0.3656	22−71	0.3656	27−78	0.417	29−83	0.4281
19−65	0.417	22−70	0.3656	27−75	0.3656	31−86	0.3842
19−62	0.4288	22−74	0.328	27−67	0.3656	31−87	0.3842
19−64	0.328	22−69	0.328	27−76	0.328	31−84	0.4197
19−69	0.0703	22−64	0.0703	27−74	0.0703		

TABLE 4: Conformational Parameters of Ara-A Obtained from X-ray Diffraction,[15] ab Initio, and PM3 Geometry Optimization

parameter	X-ray diffraction[15]	ab initio geometry optimization	PM3 geometry optimization
exocyclic torsion angles			
χ (O4′−C1′−N1−C8)	57.82° (anti)	57.18° (anti)	33.02° (anti)
γ (O5′−C5′−C4′−C3′)	178.83° (ap)	−174.10° (ap)	−172.842° (ap)
δ (C5′−C4′−C3′−O3′)	81.56	71.75°	111.25°
endocyclic torsion angles			
ν_0 (C4′−O4′−C1′−C2)	−4.38°	−20.27°	13.75°
ν_1 (O4′−C1′−C2′−C3′)	−19.01°	−4.90°	−17.34°
ν_2 (C1′−C2′−C3′−C4′)	33.53°	26.50°	14.22°
ν_3 (C2′−C3′−C4′−O4′)	−36.97°	−38.77°	−7.00°
ν_4 (C3′−C4′−O4′−C1′)	26.17°	37.29°	−4.20°
P^a	25.18°	48.26°	−32.87
$\nu_{max}{}^b$	37.05°	39.82°	16.93°
sugar pucker	$^3T_4$	$_4T^3$	$_2T^1$

[a] $\tan P = [(\nu_4 + \nu_1) - (\nu_3 + \nu_0)]/[2\nu_2(\sin 36° + \sin 72°)]$. [b] $\nu_{max} = \nu_2/\cos P$.

predict a significant vibrational coupling between the sugar and base moieties; mixed modes with considerable base and sugar contributions are observed in this region. The N−H scissoring vibration appears in this spectral region, as described previously by several authors for adenine and adenosine molecules.[20−24,26,28,38] The ab initio treatment attributes the 1661, 1644, 1613, and 1579 IR bands to the amino scissoring coupled with several CC and CN stretching motions, mainly located on the pyrimidine ring. Few differences are found between ab initio and PM3 PED predictions. Nevertheless, according to PM3 calculation, the amino scissoring does not contribute to the 1613 cm^{-1} band, and the CC and CN base stretches dominate. In the spectrum of the ara-A-d_6 isotopomer, Figure 3, two intense bands are observed at 1658 (broad) and 1614 cm^{-1} (sharper). According to both ab initio and PM3 predictions, there are important CN and CC base contributions in this region that could explain the presence of these bands in the spectrum of the isotopomer. The band at 1579 cm^{-1} of ara-A shifts to 1574 cm^{-1} and decreases in intensity by deuteration. Toyama et al.[23] ascribed this band for adenosine to N1C6 or N3C4 stretches, contributions that we also find in our ab initio and PM3 calculations. Bioviban A indicates that the 1613 cm^{-1} band is due to the C5′H_2 scissoring. Nevertheless, according to the ab initio and PM3 calculations and the results obtained for different nucleosides,[27,39] this vibration appears at lower frequencies, ≈1400−1430 cm^{-1}. The ab initio and PM3 results indicate that the IR band at 1507 cm^{-1} (1504 cm^{-1} in Raman) is mainly due to imidazole ring vibrations, and an important wavenumber shift of this band is observed upon C8 deuteration. Toyama et al.[23] found a similar result for adenosine. Imidazole ring vibrations also give rise to the weak band at 1439 cm^{-1}, predicted by ab initio calculations at 1432 cm^{-1}, in agreement with the results for adenosine.[23] The band at 1480 cm^{-1} is usually assigned to adenine motions; PM3 agrees with this assignment, but ab initio predicts dominant contributions from motions of the glycosidic region. The ab initio and PM3 calculations indicate that the bands at 1419 (IR), 1416 (Raman), and 1406 cm^{-1} (IR) have strong contributions from the methylene C5′H_2 scissoring, in agreement with previous results for nucleosides and nucleotides.[27,39,40] At 1374 cm^{-1} appears one IR band (1379 cm^{-1} in Raman) that shifts to lower wavenumbers by deuteration. Ab initio and PM3 suggest that it is due to sugar vibrations, with participation of hydroxyl groups. A strong Raman band appears at 1337 cm^{-1} (1333 cm^{-1} in IR). Different assignments have been proposed for this band in bases, nucleosides, and nucleotides. Toyama et al.[23] ascribed the band at 1330 cm^{-1} for the adenosine molecule to pyrimidine ring motions. Fodor et al.[41] attributed the 1339 cm^{-1} Raman band of 5′-dAMP to imidazole CN stretching vibrations. Theophanides et al.,[19] for the ara-A molecule, and Dahouadi et al.,[20] for adenine, assigned this band to a normal mode involving both pyrimidine and imidazole ring vibrations. The ab initio calculation attributes this band mainly to pyrimidine ring vibrations with small contributions from imidazole vibrations. The PM3 calculation predicts considerable contributions from both pyrimidine and imidazole ring vibrations. No band shift is observed in the spectrum of the ara-A-d_6 isotopomer, a result that supports the ab initio description. The strong Raman band at 1308 cm^{-1} is assigned from the ab initio and PM3 calculations to a base vibration, involving both pyrimidine and imidazole rings.[19−21,23] The IR bands at 1255, 1237, and 1148 cm^{-1} are attributed to vibrations of the sugar moiety by both methods. All these bands are drastically affected by deuteration. The band at 1218 cm^{-1} in IR and 1215 cm^{-1} in Raman shows a high contribution of in plane C_8−H bend (ab initio). This proposal agrees with other results[23] and is supported by the isotopic shift observed upon deuteration. Imidazole contributions are also found for the band at 1180 cm^{-1}, with a remarkable participation of the N9−C1′ stretch.[23] The IR bands at 1132, 1103, 1087, 1055, and 1033 cm^{-1} are almost pure sugar vibrations,[23] and a relevant contribution of the amino rocking[21,28] (35%) is obtained for the IR band at 1007 cm^{-1}.

Below 1000 cm^{-1}. In this spectral region the normal modes tend to be less localized and the sugar-base vibrational coupling increases. The IR bands at 983 and 921 cm^{-1} are due to almost pure sugar vibrations. The latter may be described as a sort of arabinose ring breathing vibration.[27] The weak IR and Raman band at 953 cm^{-1} is assigned to several out-of-plane bends, opb's, coupled with sugar motions; the opb H−C2N is one of the most relevant contributions.[20,23] The opb H−C8 is predicted by both methods at 841 cm^{-1}, in agreement with the neutron inelastic scattering, NIS, results for the adenine.[20] The group of strong Raman bands at 803, 732, and 706 cm^{-1} have important contributions of several base stretches and bends, and it is possible to speak of a kind of "base breathing modes". The band at 687 cm^{-1} is ascribed by PM3 to vibrations of the amino group, while the ab initio treatment proposes several base torsions (mainly of the C8−N7 bond). Dhaouadi et al.[20] describe at this frequency a mode for the adenine composed by several opb's and torsions, including C8N9 and C8N7. Dominant base contributions are found for the bands at 629, 577, 542, and 526 cm^{-1} by both methods, while motions of the sugar and base moieties are associated with the bands at 595, 296, 283, 224, and 128 cm^{-1}.

Sugar vibrations are the main origin of the bands at 563, 507 (with a considerable contribution of the bend of the glycosidic bond), and 459 cm^{-1}. The sugar moiety also, with dominant contributions from CO torsions, gives rise to the 360, 334, 324, 305, and 265 cm^{-1} bands. CC sugar torsions contribute to the 178, 166, 128, 101, 83, and 45 cm^{-1} bands.

The C6−N6 amino torsion is calculated by HF/3-21G at 433 cm^{-1}. PM3 locates the higher contribution of this torsion (88%) at 324 cm^{-1}, corresponding to a strong IR band that disappears upon deuteration. This assignment agrees with previous NIS results for adenine.[20] The rest of the bands may be ascribed to complex and delocalized vibrations (crystal lattice vibrations and torsions appear in this spectral region) involving the whole molecule. The glycosidic bond torsion is calculated at 20 cm^{-1} (ab initio) and 17 cm^{-1} (PM3). Hydrogen bond and crystal

lattice modes, appearing in this region, are not predicted by the computational methods used.

Conclusions

It has been observed that the transference of force constants coming from related molecules, without refining, leads to a rough approximation (calculation A). This fact points out the significance of the interactions among the different fragments and the changes induced in the force constants by these interactions. A better agreement is found when the transferred force field comes from a calculation (ab initio in this case) performed on the whole molecule (calculation B), but the results do not reach the accuracy obtained from scaled PM3 or scaled ab initio treatments.

The scaling procedure tends to correct the inherent errors of these methods and those from the approximation to the sample conditions. The wavenumbers obtained from the scaled ab initio HF/3-21G calculation are in very good agreement with the observed wavenumbers in most cases (standard deviation 6.16 cm^{-1}), and the scaled PM3 calculation provides a reasonable approximation (standard deviation 12.0 and 6.74 cm^{-1} without considering four CH stretching frequencies).

Acknowledgment. The authors are grateful to Bruker Española, FTIR/FT-Raman Division, for the use of their FT-Raman equipment, and to Mr. Delgue and Mr. Boulou for their valuable help.

The 2232 transferred force constants to build the valence force field are given in Table 1S. The observed (FTIR and FT-Raman) and calculated (scaled ab initio HF/3-21G, PM3, Bioviban A and B) wavenumbers for ara-A molecule are listed in Table 2S (HF/3-21G and PM3) and Table 3S (Bioviban A and B) (50 pages). Ordering information is given on any current masthead page. The complete scaled ab initio HF/3-21G force field in Gaussian 94 F_x format may be obtained from the authors on request.

References and Notes

(1) Saenger, W.; Cantor, R. C. *Principles of Nucleic Acids Structure*; Spinger-Verlag: New York, 1984; p 55.

(2) Lee, W. W.; Benitez, A.; Goodman, L.; Baker, B. R. *J. Am. Chem. Soc.* **1960**, *82*, 2648.

(3) Hertzberg, R. P. In *Comprehensive Medicinal Chemistry. The Rational Design, Mechanistic Study & Therapeutic Application of Chemical Compounds*, Vol. 2. *Enzymes & Other Molecular Targets*; Hansch, C., Sammes, P. G., Eds.; Pergamon Press: Oxford, 1990; pp 753−791.

(4) Müller, F. A.; Dixon, G. J.; Ehlich, J. In *Antimicrobial Agents and Chemotherapy*; Hobby, G. I., Ed.; American Society for Microbiology: Bethesda, 1969; pp 136−147.

(5) DeClercq, E. *Antimicrob. Agents Chemother.* **1982**, *21*, 661.

(6) Collins, P.; Bauer, D. J. *Ann. NY Acad. Sci.* **1977**, *284*, 49.

(7) Rossi, A. In *Nucleoside Analogues. Chemistry, Biology and Medical Applications*; Walker, R. T., DeClercq, E., Erkstein, F., Eds.; Plenum Press: New York, 1979; pp 409−436.

(8) Nicholson, K. G. *Lancet* **1984**, 503.

(9) Montgomery, J. A.; Johston, T. P.; Shealy, Y. F. *Burger's Medicinal Chemistry*, 4th ed.; Wolff, M. E., Ed.; John Wiley: New York, 1979; Part II, pp 595−670.

(10) Iliakis, G.; Pantelias, G. E.; Seaner, R. *Radiat. Res.* **1988**, *114*, 361.

(11) (11) Wilman, D. E. *The Chemistry of Antitumor Agents*; Blackie: Glasgow, 1990; p 304.

(12) (12) Suhadolnik, R. J. *Nucleoside Antibiotics;* Wiley-Interscience: New York, 1970; Chapter 3.

(13) DeClercq, E. *Acta Microbiol. Acad. Sci. Hung.* **1981**, *28*, 289.

(14) Müeller, W.; Rodhe, H.; Beyer, R.; Maindhorf, A.; Lanchmann, M.; Tascher, H.; Zahn, R. *Cancer Res.* **1975**, *35*, 2160.

(15) Bunick, G.; Voet, D. *Acta Crystallogr. B* **1974**, *30*, 1651.

(16) Orza, J. M.; Escribano, R.; Navarro, R. *J. Chem. Soc., Faraday Trans.* **1984**, *2*, 653.

(17) Cohen, S. S. *Prog. Nucl. Acid Res. Mol. Biol.* **1966**, *5*, 1.

(18) Escribano, R. Ph.D. Thesis, University Complutense, Madrid, 1976.

(19) Theophanides, T.; Hanessian, S.; Manfait, M.; Berjot, M. *J. Raman Spectrosc.* **1985**, *16*, 32.

(20) Dhaouadi, Z.; Ghomi, M.; Austin, J. C.; Girling, R. B.; Hester, R. E.; Mozjes, P.; Chinsky, L.; Turpin, P. Y.; Coulombeau, C.; Jobic, H.; et al. *J. Phys. Chem.* **1993**, *97*, 1074.

(21) Majoube, M.; Millié, P.; Lagant, P.; Vergoten, G. *J. Raman Spectrosc.* **1994**, *25*, 821.

(22) Nowak, M. J.; Lapinski, L.; Kwiatkowski, J. S.; Leszczynski, J. *J. Phys. Chem.* **1996**, *100*, 3527.

(23) Toyama, A.; Hanada, N.; Takeuchi, H.; Harada, H.; Abe, Y. *J. Raman Spectrosc.* **1994**, *25*, 623.

(24) Mohan, S.; Ilangovan, V. *Indian J. Pure Appl. Phys.* **1993**, *31*, 750.

(25) Majoube, M. *J. Raman Spectrosc.* **1985**, *16*, 98.

(26) Bertoluzza, A.; Fagnano, R.; Tosi, R.; Morelli, M. A.; Long, D. A. *J. Raman Spectrosc.* **1987**, *18*, 83.

(27) Tsuboi, M.; Ueda, T.; Ushizawa, K.; Sasatake, Y.; Ono, A.; Kainosho, M.; Ishido, Y. *Bull. Chem. Soc. Jpn.* **1994**, *67*, 1483.

(28) Tsuboi, M.; Nishimura, Y.; Hirakawa, A. Y.; Peticolas, W. L. In *Biological Applications of Raman Spectroscopy*, Vol. 2. *Resonance Raman of Polyenes and Aromatics*; Spiro, T. G., Ed.; John Wiley: New York, 1987; pp 109−179.

(29) Bailey, L. E.; Hernanz, A.; Navarro, R.; Theophanides, T. *Eur. Biophys. J.* **1996**, *24*, 149.

(30) Bailey, L. E.; Navarro, R.; Hernanz, A. *Biospectroscopy* **1997**, *3* , 47.

(31) Frisch, M.; Trucks, G.; Head-Gordon, M.; Gill, P.; Wong, M.; Foresman, B.; Johnson, H.; Shlegel, H.; Robb, M.; Gomperts, J.; Andres, J.; Raghavachari, K.; Binkley, J.; Gonzales, C.; Martin, R.; Fox, D.; Defrees, D.; Baker, J.; Stewart, J.; Popple, J. *GAUSSIAN 92*; Gaussian, Inc.: Pittsburgh, PA, 1992.

(32) Allouche, A.; Pourcin, J. *Spectrochim. Acta* **1993**, *49A* , 571.

(33) Wilson, E. B.; Decius, J. C.; Cross, P. C. *Molecular Vibrations*; McGraw-Hill: New York, 1955.

(34) Ghomi, M.; Taillandier, E. *Eur. Biophys. J.* **1985**, *12*, 153.

(35) Palmö, K.; Pietilä, P. O.; Mannfors, B. *Croat. Chem. Acta* **1988**, *61*, 605.

(36) Pulay, P. *J. Mol. Struct.* **1995**, *347*, 293.

(37) Eyster, J.; Prohofsky, E. W. *Spectrochim. Acta* **1974**, *A30*, 2041.

(38) Tsuboi, M.; Takahasi, S.; Harada, I. In *Physico-Chemical Properties of Nucleic Acids*, Vol. 2. *Structural Studies on Nucleic Acids and Other Biopolymers*; Duchesne, J., Ed.; Academic Press: London, 1973; pp 91−145.

(39) Lord, R. C.; Thomas, G. J., Jr. *Spectrochim. Acta* **1967**, *23A*, 2551.

(40) Thomas, G. J., Jr.; Tsuboi, M. In *Advances in Biophysical Chemistry*, Vol. 3; Allen Bush, C., Ed.; Jai Press Inc.: Greenwich, CT, 1993; pp 1−70.

(41) Fodor, J.; Rava, R. P.; Hays, T. R.; Spiro, T. G. *J. Am. Chem. Soc.* **1985**, *107*, 1520.